Supporting Information

Novel Deep Blue Hot Exciton Material for High-Effeciency Nondoped Organic Light-Emitting Diode

Pei Xu, [a] *Lei Xu,* [a] *Yuyu Pan,*[c] *Dezhi Yang,*[a] *Zetong Ma,*[a] *Xianfeng Qiao,* [a] *Dehua Hu,** [a,b] *Dongge Ma,* [a] *and Yuguang Ma** [a]

[a] State Key Laboratory of Luminescent Materials and Devices, South China University of Technology, Guangzhou, 510640, P. R. China

[b] School of Chemical Engineering and Light Industry, Guangdong University of Technology, Guangzhou 510006, China.

[c] Shenyang Univ Technol, Sch Petrochem Engn, 30 Guanghua St, Liaoyang 111003, P. R. China

E-mail: msdhhu@scut.edu.cn; ygma@scut.edu.cn

Contents

S1. Synthesis General

The ^{1}H NMR spectra was recorded on a Bruker AVANCE 500 spectrometer at 500 MHz, using tetramethylsilane (TMS) as the internal standard and $CDCl_3$ as the solvent. The matrix- assisted laser desorption ionization time-of-flight (MALDI-TOF) mass spectrum was measured using an AXIMA-CFRTM plus instrument.

^{1}H NMR (500 MHz, Chloroform-d) δ 8.04 (t, J = 1.7 Hz, 1H), 7.93 (d, J = 6.5 Hz, 2H), 7.91 - 7.86 (m, 2H), 7.78 - 7.70 (m, 6H), 7.66 - 7.61 (m, 2H), 7.59 - 7.53 (m, 2H), 7.47 (t, J = 7.6 Hz, 4H), 7.42 - 7.35 (m, 6H).^{13}C NMR (101 MHz, $CDCl_3$) δ 143.48, 140.89, 139.67, 138.65, 136.93, 133.66, 131.30, 131.26, 128.81, 128.40, 127.88, 126.65, 126.28, 125.03, 124.77, 124.39, 124.22, 117.89, 110.62.

MALDI-TOF-MS (m/z): calcd for $C_{39}H_{25}N$, 507.20; found, 507.28 [M+].

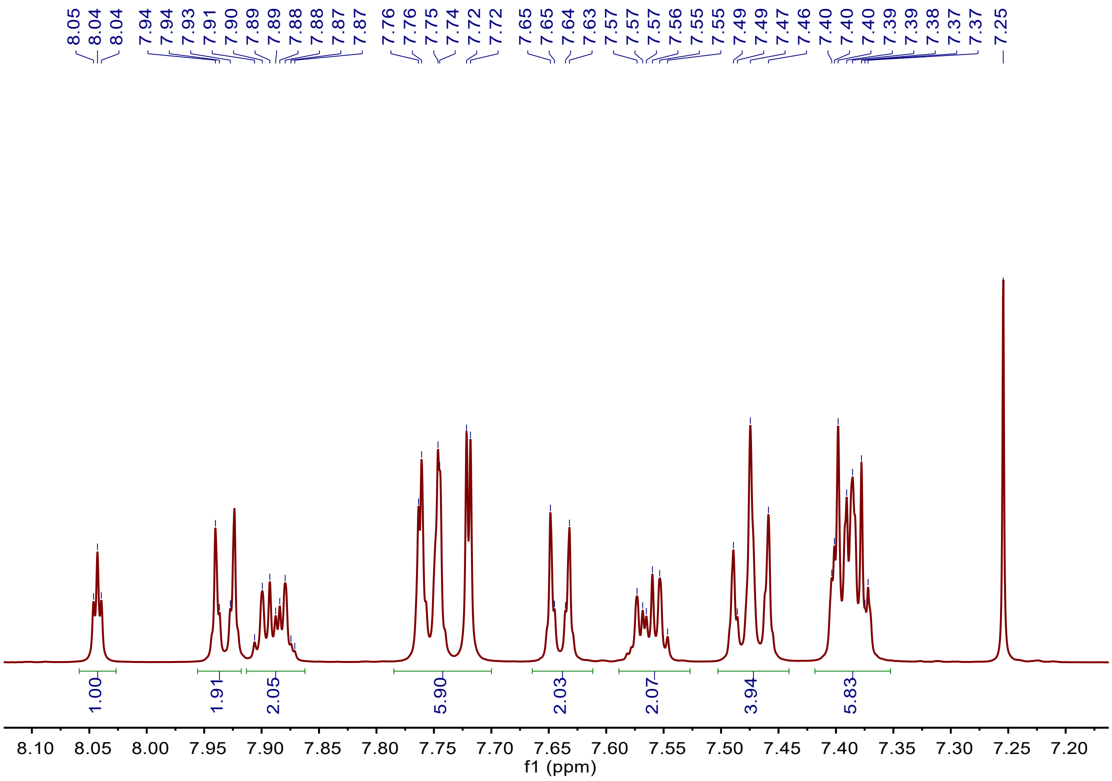

Figure S1. ^{1}H-NMR Spectrum of MACN in $CDCl_3$.

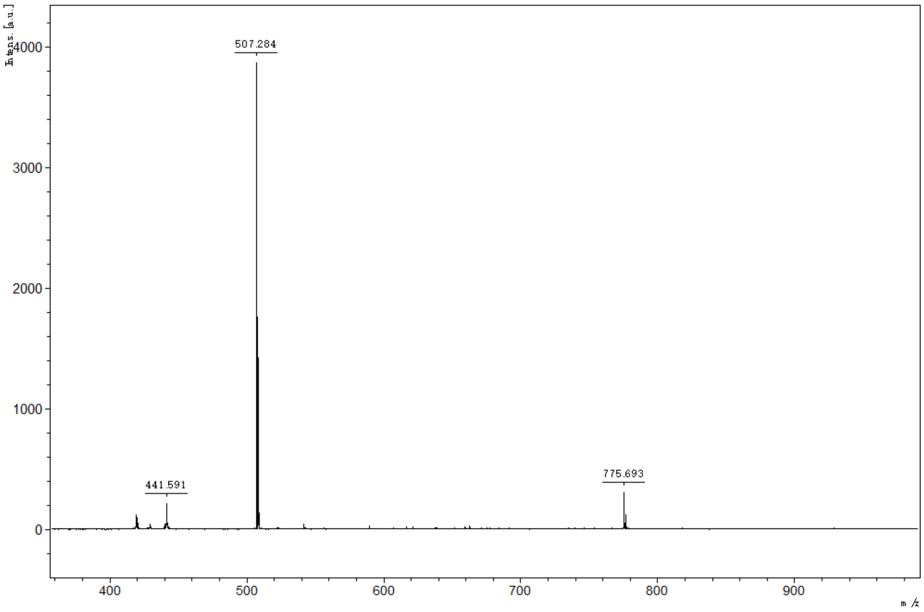

Figure S2. Mass Spectrum (M+H+) of MACN.

S2. Supplementary Thermal and Electrochemical Properties

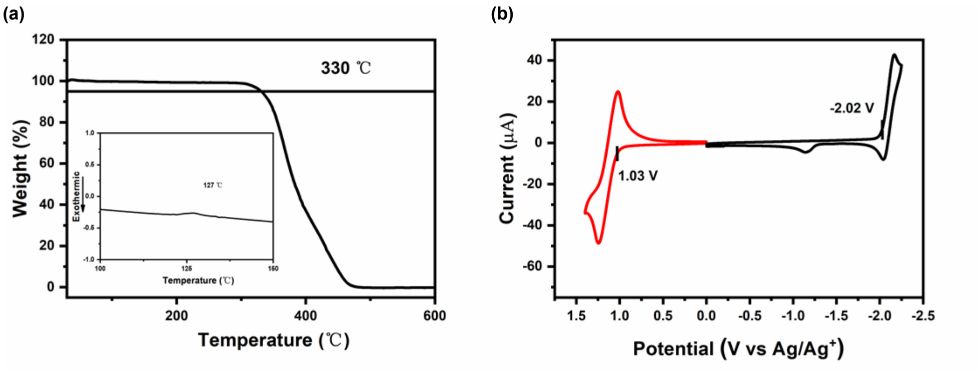

Figure S3. (a) TGA and DSC curves (inset) of MACN. (b) Electrochemical CV curves of MACN.

S3. Supplementary Theoretical Calculations

	Singlets				Triplets		
	Hole		Particle		Hole		Particle
$S_0 \rightarrow S_1$	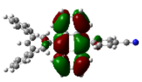	**98.60%**	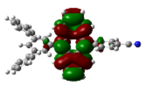	$S_0 \rightarrow T_1$	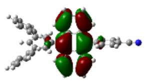	**96.89%**	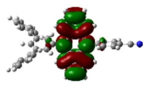
$S_0 \rightarrow S_2$	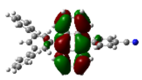	**50.12%**	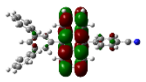	$S_0 \rightarrow T_2$	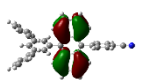	**57.21%**	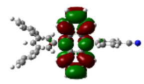
$S_0 \rightarrow S_3$	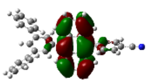	**99.84%**	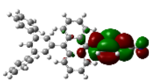	$S_0 \rightarrow T_3$	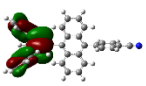	**64.01%**	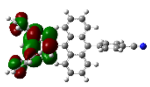

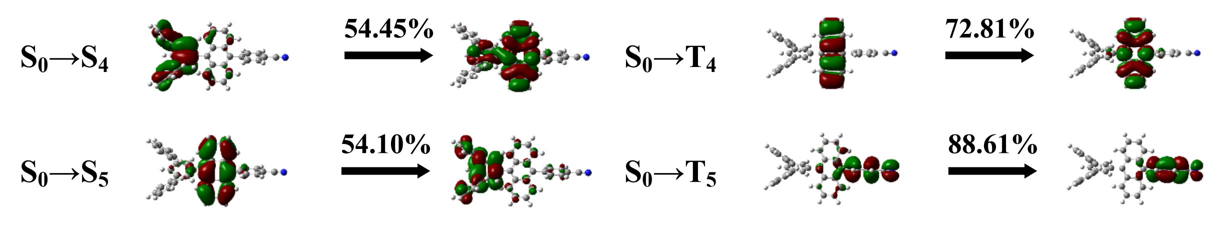

Figure S4. The NTO transition character of the first five singlet and triplet states.

S4. Supplementary Photophysical Properties

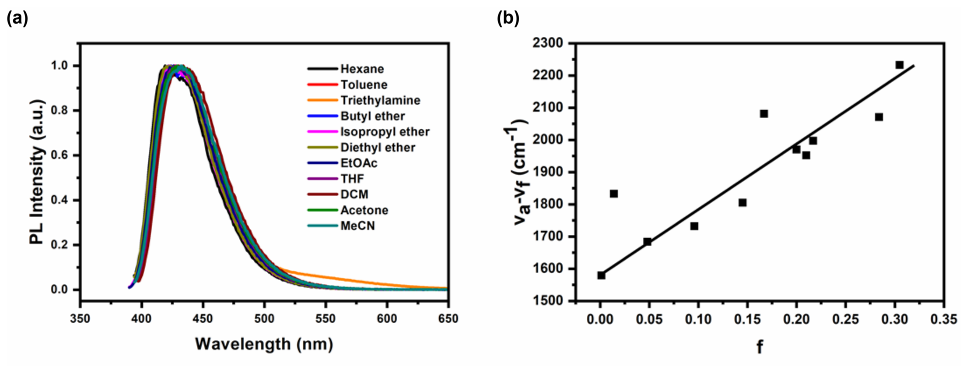

Figure S5. (a) PL spectra in different solvents; (b) Lippert–Mataga plots of the fluorescence maxima of MACN against the solvent polarity parameters

Table S1. Photophysical parameters of MACN

MACN	PLQY **(%)**	τ(ns)	$K_r/10^8(S^{-1})$	$K_{nr}/10^8(S^{-1})$
THF	74.3	4.26	1.74	0.61
Neat film	38.2	1.04	3.67	5.95

S5. Supplementary Electroluminescence Performances

To evaluate the transporting properties of this material, single-carrier devices were fabricated with structure of ITO/NPB (10 nm)/MACN (80nm)/NPB (10 nm)/Al for hole-only device and ITO/TPBi (10 nm)/MACN (80 nm)/TPBi (10 nm)/LiF /Al for electron-only device. NPB and TPBi are used to prevent electron and hole injection from the cathode and anode, respectively. As the voltage increased, the current becomes space-charge limited with a nearly quadratic dependence on voltage. The hole and electron mobilities were calculated from the slope of the $J^{1/2}$-V curves to be 1.47×10^{-12} $cm^2\ V^{-1}s^{-1}$ and 6.13×10^{-7} $cm^2\ V^{-1}\ s^{-1}$, respectively, indicating that imbalance of carrier recombination may be the reason for limiting the EQE of devices based on MACN.

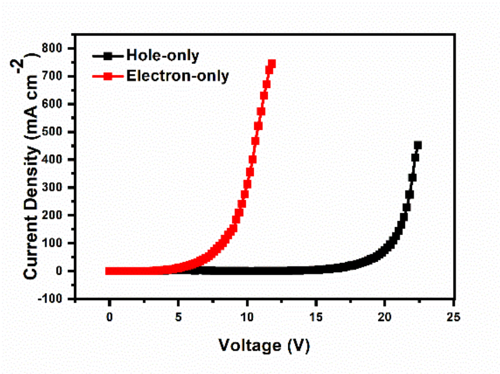

Figure S6. Current density versus voltage characteristics of the hole-only and electron-only devices.

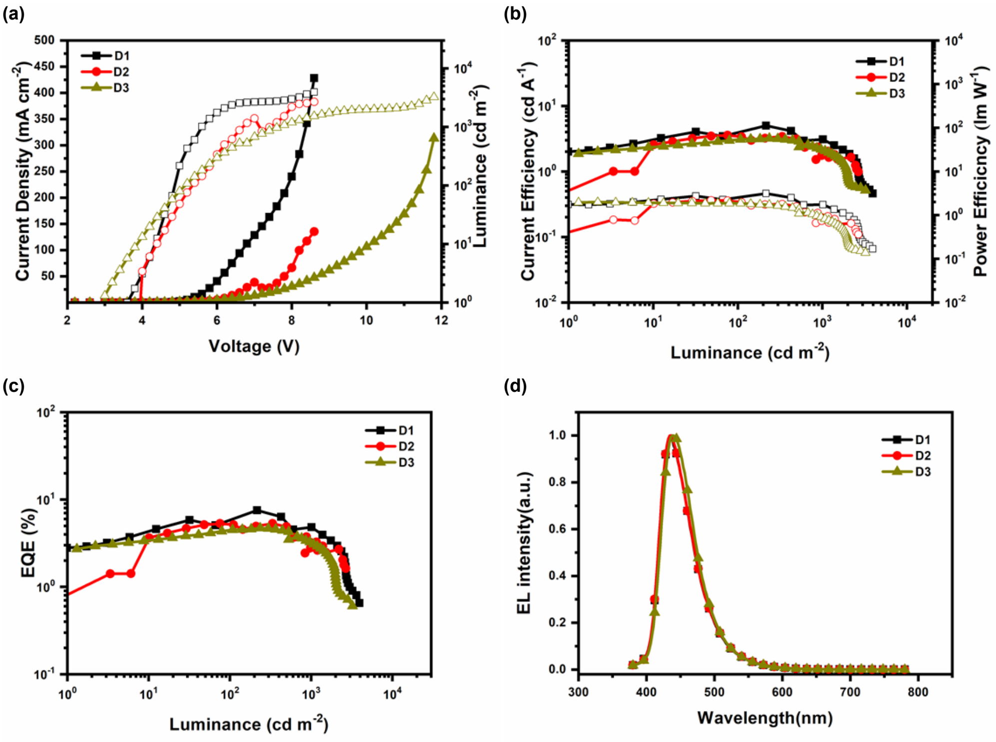

Figure S7. (a) J-V-L curves of the devices. (b) CE-L-PE characteristics. (c) L-EQE curves. (d) The EL spectra.

Table S2. Device performances of MACN OLEDs with different structures

Device	V_{on} (V)	L_{max} (cd m^{-2})	CE_{max} (cd A^{-1})	EQE_{max} (%)	PE_{max} (lm W^{-1})	EL peak (nm)	CIE (x,y)
A	3.8	3942	4.99	7.51	3.14	436	(0.154,0.075)
B	4	2682	3.56	5.31	2.94	436	(0.155,0.075)
C	3	3236	3.21	4.71	1.99	438	(0.153,0.75)

Device A: ITO/ PEDOT: PSS (40 nm)/TCTA (40 nm)/MACN (20 nm)/ TPBi (30 nm)/LiF/Al

Device B: ITO/P PEDOT: PSS (40 nm)/TCTA (40 nm)/MACN (20 nm)/TmPyPb (30 nm)/LiF/Al

Device C: ITO/ PEDOT: PSS (40 nm) /TAPC (20 nm) /TCTA (30 nm)/MACN (20 nm)/TPBi (30 nm)/LiF/Al

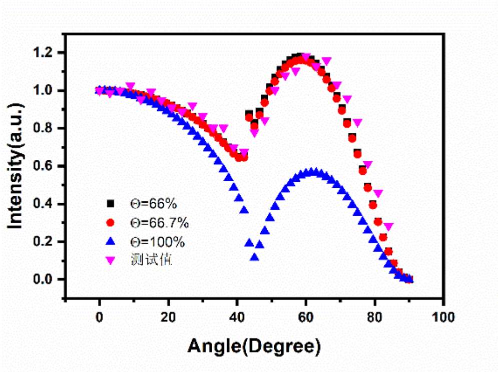

Figure S8. Variable-angle PL measurements of MACN film. Θ, orientation factors. For fully horizontal dipoles, Θ equals 100% and isotropic dipole orientation, Θ equals 67%.

S6. Supplementary Mechanism Study

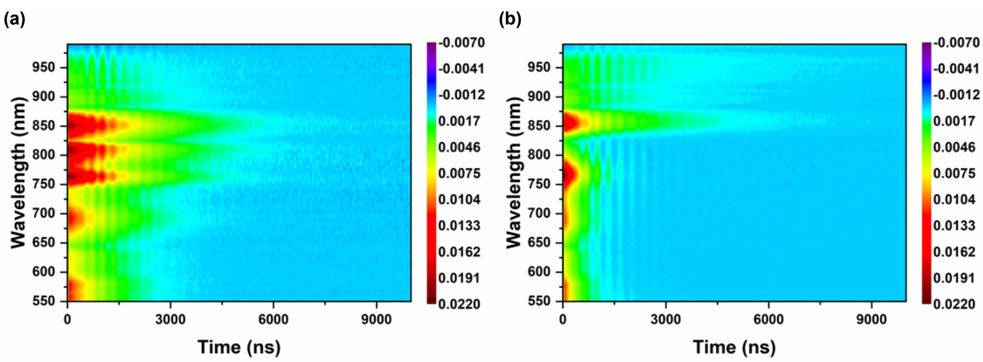

Figure S9. (a) Transient absorption spectra of the pristine PtOEP solution. (b) Transient absorption spectra of the MACN & PtOEP solution.

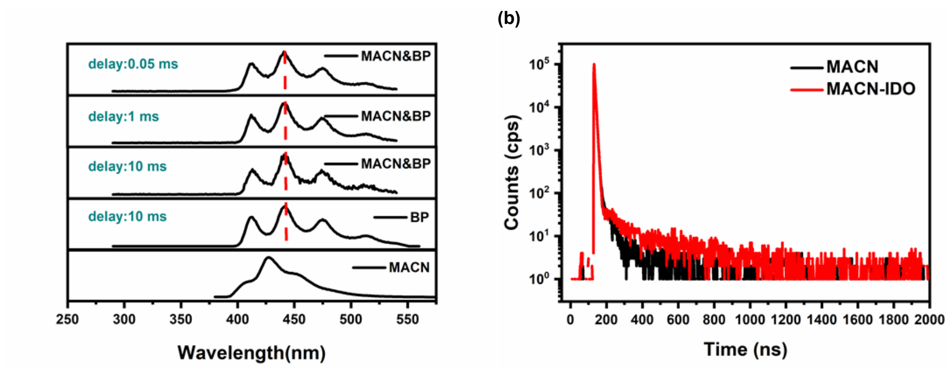

Figure S10. (a) Top: the delayed emission spectrum of the MACN & BP solution; middle: the phosphorescence spectrum of BP. The fluorescence spectrum of MACN at 77 K appears at the bottom. In the mixed solution, the concentration of the ketones was 10^{-5} M, and the concentration of MACN was 10^{-4} M. The excitation wavelength was 280 nm. (b) The PL decay spectra of the MACN and MACN& IDO solutions at room temperature.